

[View Journal Online](#)  
[View Article Online](#)

## Molecular mechanistic vision on binding interaction of triptan drug, a serotonin (5-HT<sub>1</sub>) agonist with human serum albumin through multispectral and computational assessments

Manjushree Makegowda  and Revanasiddappa Hosakere Doddarevanna  \*

Department of Chemistry, University of Mysore, Manasagangothri, Mysuru 570006, Karnataka, India  
mmanjushreem@gmail.com (M.M.), hdrevanasiddappa@yahoo.com (R.H.D.)

\* Corresponding author at: Department of Chemistry, University of Mysore, Manasagangothri, Mysuru 570006, Karnataka, India.  
e-mail: [hdrevanasiddappa@yahoo.com](mailto:hdrevanasiddappa@yahoo.com) (R.H. Doddarevanna).

### RESEARCH ARTICLE



doi: [10.5155/eurjchem.11.2.145-155.1971](https://doi.org/10.5155/eurjchem.11.2.145-155.1971)

Received: 14 February 2020

Received in revised form: 24 March 2020

Accepted: 26 March 2020

Published online: 30 June 2020

Printed: 30 June 2020

### ABSTRACT

The triptan drug such as eletriptan in combination with hydrochloride (ETP) is a 5-HT<sub>1</sub> receptor agonist used to treat the migraine headache. Human serum albumin (HSA), the fundamental serum protein, executes various functions, that includes transporting and binding of many ligands. HSA binding interaction with ETP is elucidated from molecular docking in composite with fluorescence (emission, 3D and synchronous), UV-vis and FT-IR spectroscopy at 296, 304 and 312 K (pH = 7.40). ETP after interaction modified the HSA secondary structure and its micro-environments. Energy transfer and thermodynamic parameters were evaluated. Various quenching and binding constants were computed for formed ETP-HSA complex. The dominant interactive forces for ETP and HSA binding are hydrogen bonds join up with van der Waals extent possibly at site III (IB). The presence of Ca<sup>2+</sup>, Co<sup>2+</sup>, Na<sup>+</sup>, Mg<sup>2+</sup> and Fe<sup>3+</sup> ions significantly affected binding ability of ETP towards HSA. The essentialness of this investigation is beneficial in life sciences, medicinal chemistry, pharmaceutical industry and clinical medicine.

### KEYWORDS

Eletriptan  
Energy transfer  
Molecular docking  
Binding interaction  
Secondary structure  
Fluorescence quenching

Cite this: Eur. J. Chem. 2020, 11(2), 145-155

Journal website: [www.eurjchem.com](http://www.eurjchem.com)

### 1. Introduction

The severe outcome of cyclic headaches of moderate level, causes the migraine. Typically, about 15% world populations are affected by this disorder where it starts and becomes worst at puberty and middle age, respectively. Majorly, females are less affected than males. The main reasons for migraines are change in hormone level, genetic and environmental factors. Usually migraines occur in nature at one side of the head which involves the blood vessels and nerves of the brain with pulse to three days. This pain has common symptoms namely vomiting, nausea and sensitivity to smell or sound or light which leads to loss of physical activity. One of the best second generation triptan drugs for the treatment of migraine is eletriptan which is often used in combination with hydrochloride namely eletriptan hydrochloride (ETP) (Figure 1a). This drug was approved by U. S. Food and Drug Administration (FDA). ETP is a serotonin receptor agonist, particularly to family of 5-HT<sub>1</sub> receptor agonist. The blood vessels sore around the brain is to be reduced during the migraine of head pain by ETP. ETP should not give to the patients having diseases like heart related problems and stroke. Moreover, it has common advert effects

such as somnolence, nausea, hypertension, asthenia, dizziness and this side effect increases with dose [1-3].

Serum albumins are bind by drug in blood may strongly influence drugs distribution, metabolism, absorption, excretion and its transportation [4]. Bioavailability and circulating lifetimes of drug could be determined from drug binding affinity to protein. Weak interactions result in inadequate distribution and reduce the lifetimes while strong one diminishes the drug free fraction in plasma. There is necessary to establishing a balance between drugs's free and bound type to obtain precise therapeutic doses, hence reasonable amounts could be supplied to targeted tissues and to reduce noxious side effects.

Broadly utilized protein i.e. serum albumins in drug binding investigations is human serum albumin (HSA) (Figure 1b) where it assists to maintain neutralize toxins and intravascular colloid osmotic pressure [5]. The heart shaped HSA been constituted with three homologous domains [6].

ETP binding to HSA at 296, 304 and 312 K was investigated via various spectroscopic and docking methods. Effects of Ca<sup>2+</sup>, Co<sup>2+</sup>, Na<sup>+</sup>, Mg<sup>2+</sup> and Fe<sup>3+</sup> ions were also examined. On the basis of literature observe [7-15], this work has not been done.

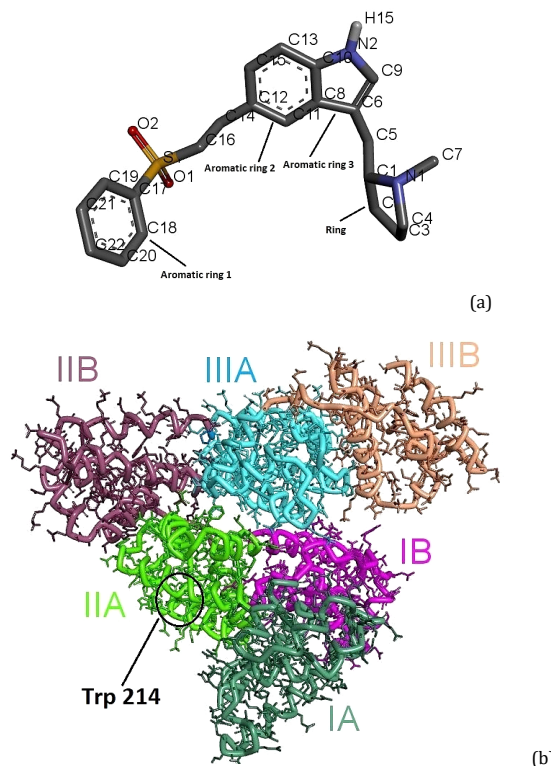


Figure 1. (a) ETP and (b) HSA 3D structure.

## 2. Experimental

### 2.1. Reagents and stocks

Human serum albumin (Lyophilized powder, fatty acid free, globulin free, ≥99%; agarose gel electrophoresis), calcium chloride hexahydrate ( $\text{Ca}^{2+}$ , 98%), cobalt(II) chloride hexahydrate ( $\text{Co}^{2+}$ , ≥97%), sodium chloride ( $\text{Na}^+$ , ≥99%), magnesium sulfate heptahydrate ( $\text{Mg}^{2+}$ ; ≥97%), iron(III) oxalate hexahydrate ( $\text{Fe}^{3+}$ ), warfarin (analytical standard), digitoxin (≥92%) and ibuprofen (≥98%) were products of Sigma-Aldrich (USA). Analytical standards were employed for other exploited chemicals. Tris buffer was made from double-distilled water at pH = 7.40 where this was executed throughout every experiment by simultaneously corrected its background. Concentration of  $1.0 \times 10^{-4}$  mol/L for HSA and  $1.0 \times 10^{-3}$  mol/L for site probes, ETP and metal ions as stocks.

### 2.2. UV-vis absorption study

Absorbance estimations (200-300 nm) at 304 K were executed on Life Sciences DU 730: UV-visible Spectrophotometer (Beckman Coulter, U.S.A) for HSA ( $2.70 \times 10^{-6}$  mol/L) with increased ETP solution (0.0 to  $4.50 \times 10^{-6}$  mol/L about each increment of 0.45).

### 2.3. FT-IR spectral observations

Free HSA ( $2.70 \times 10^{-6}$  mol/L) and ETP-HSA system's FT-IR spectra at 304 K were conducted from FT-IR spectrometer (Spectrum Two, Perkin Elmer, USA) in 1700-1500  $\text{cm}^{-1}$  region where ETP concentration was  $2.70 \times 10^{-6}$  mol/L. ORIGINPRO 9.0 Software analyzed the curve fitting measurements to secondary structures.

### 2.4. Emission fluorescence

Fluorescence estimations were implemented on fluorescence spectrophotometer (F-4600, Hitachi, Japan) with 10 nm

(excitation/emission) slit width. HSA was  $2.70 \times 10^{-6}$  mol/L with different ETP (0 to  $4.50 \times 10^{-6}$  mol/L) concentrations with  $\lambda_{em} = 290\text{-}420$  nm and  $\lambda_{ex} = 295$  nm at 296, 304 and 312 K. Absorbance of ETP at emission ( $A_{em}$ ) and excitation ( $A_{ex}$ ) wavelengths was noted down to decline the effects from inner filter for entire fluorescence intensities of HSA ( $F_{obs}$  = observed and  $F_{cor}$  = corrected) [16].

$$F_{cor} = F_{obs} \times e^{(A_{ex} + A_{em})/2} \quad (1)$$

### 2.5. Synchronous fluorescence

These spectra were noted down at 304 K in 210-320 nm for ETP-HSA system. Concentration of HSA persisted at  $2.70 \times 10^{-6}$  mol/L while ETP differed from 0 to  $4.50 \times 10^{-6}$  mol/L.

### 2.6. Energy transfer between ETP and HSA

HSA ( $2.70 \times 10^{-6}$  mol/L) emission and ETP absorption spectrum ( $2.70 \times 10^{-6}$  mol/L) were recorded at 304 K in 290-420 nm. These two overlapping determine the efficient energy transfer.

### 2.7. Metal ions on ETP-HSA binding

HSA ( $2.70 \times 10^{-6}$  mol/L) fluorescence spectra with  $\text{Ca}^{2+}$ ,  $\text{Co}^{2+}$ ,  $\text{Na}^+$ ,  $\text{Mg}^{2+}$  and  $\text{Fe}^{3+}$  ions ( $2.70 \times 10^{-6}$  mol/L) by increased ETP amounts from 0 to  $4.50 \times 10^{-6}$  mol/L at 304 K were recorded.

### 2.8. Displacement of ETP by site selective assess

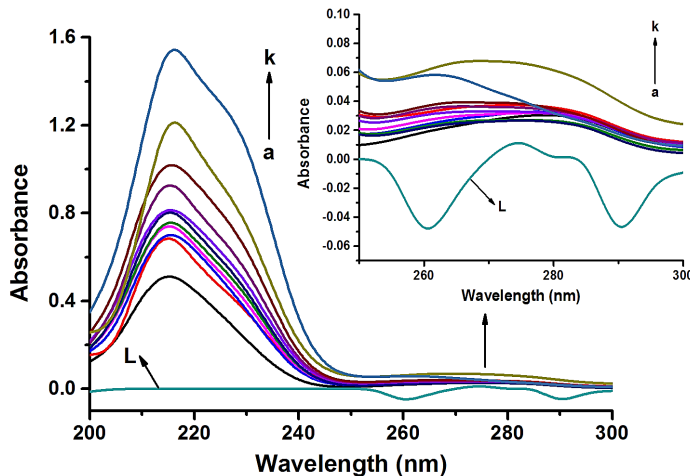
ETP displacement was monitored using warfarin (for IIA), ibuprofen (for IIIA) and digitoxin (for IB) site probes. Presence of site probes ( $2.70 \times 10^{-6}$  mol/L) with increased ETP (0 to  $4.50 \times 10^{-6}$  mol/L) concentration, HSA ( $2.70 \times 10^{-6}$  mol/L) fluorescence spectra were summarized at 304 K.

**Table 1.** FT-IR spectral aspects at 304 K.

System	Amide I ( $\text{cm}^{-1}$ )					Amide II ( $\text{cm}^{-1}$ )
	1615-1637	1638-1648	1649-1660	1660-1680	1680-1692	
Free HSA	1635 $\pm$ 0.40	1644 $\pm$ 0.90	1658 $\pm$ 0.38	1680 $\pm$ 0.63	1687 $\pm$ 0.72	1548
ETP-HSA	1627 $\pm$ 0.31	1641 $\pm$ 0.59	1657 $\pm$ 0.44	1666 $\pm$ 0.26	1682 $\pm$ 0.43	1543 $\pm$ 0.13 1538 $\pm$ 0.88

**Table 2.** Evaluated secondary structures (FT-IR) at 304 K.

System	Secondary structures (%)				
	$\beta$ -sheet	Random coil	$\alpha$ -helix	$\beta$ -turn	$\beta$ -antiparallel
Free HSA	7.00 $\pm$ 0.06	24.24 $\pm$ 0.03	50.75 $\pm$ 0.08	13.81 $\pm$ 0.10	4.19 $\pm$ 0.03
HSA-ETP	0.89 $\pm$ 0.05	15.15 $\pm$ 0.02	42.03 $\pm$ 0.05	34.34 $\pm$ 0.04	7.78 $\pm$ 0.09

**Figure 2.** Spectrum of UV-vis absorption of HSA ( $2.70 \times 10^{-6}$  mol/L) in addition of ETP ( $0$  to  $4.50 \times 10^{-6}$  mol/L): curve L is ETP alone ( $2.70 \times 10^{-6}$  mol/L) at 304 K.

### 2.9. Docking studies

Docking analysis for binding mode between ETP and HSA was executed on Autodock Tools to three binding sites. Energy minimization for 3D structures of ETP (PubChem CID 121596618) and HSA (PDB ID: 1AO6) were achieved according to Marvin View and GROMOS96 force field. Lamarckian genetic algorithm with 60 grid maps was applied and binding visualization made on Discovery Studio software.

### 2.10. 3D fluorescence

3D fluorescence of HSA ( $2.70 \times 10^{-6}$  mol/L) and ETP-HSA system at 304 K were measured. Concentration of ETP was kept at  $81.0 \times 10^{-6}$  mol/L with  $\lambda_{em} = 250$ -500 nm and  $\lambda_{ex} = 200$ -380 nm.

## 3. Results and discussion

### 3.1. UV-vis measurements

Complexation and structural modifications are exploited from UV-vis spectroscopy for protein-drug binding [17]. Responsible characteristic peaks are at 214 nm ( $n \rightarrow \pi^*$  transitions: amide cluster) and at 278 nm ( $\pi \rightarrow \pi^*$  transitions: Tyr and Trp residues) gathered for HSA over ETP interaction in UV-vis spectrum (Figure 2). Herein, these peaks suffer red shift that manifesting the altered secondary structure together with polarity in microenvironments (Tyr/Trp) of HSA. Accordingly, increased in absorbance as ETP increased concentration at each peaks of HSA dictates the formation of ETP-HSA complex.

### 3.2. FT-IR spectroscopy

Further evidence of ETP-HSA interaction was affirmed by FT-IR out comes from characteristic amide bands where amide I ( $\text{C=O}$  stretch:  $1700$ - $1600$   $\text{cm}^{-1}$ ) and II (associated C-N stretch across N-H bend:  $1600$ - $1500$   $\text{cm}^{-1}$ ) have direct replicate of HSA

secondary structure. Spectral variations noticed from Table 1 signify that ETP modified the HSA conformations (Figure 3). Curve-fitting operations with second derivative to infrared self-deconvolution were subjected to amide I (high compassion to weak conformational alterations) band to measure free HSA and its ETP complex secondary structures (Figure 4). Upon ETP interaction, a decrease of random coil,  $\alpha$ -helix and  $\beta$ -sheets with increment in  $\beta$ -turns and antiparallel were noticed for HSA (Table 2). This is indicative of a biased unfolding of HSA in ETP [18].

### 3.3. Fluorescence quenching

Decreased remarkable fluorescence intensity (blue shift  $\sim 3$  nm at 329 nm) was found for HSA by varying of ETP amounts evidenced from Figure 5 at 304 K. Decreased polarity, change and less hydrophilic of Trp ( $\lambda_{ex} = 295$  nm and  $\lambda_{em} = 340$  nm) micro-environment might exhibited from this blue shift. This ensures that ETP bound to HSA with high affinity by efficiently quenched the HSA intrinsic fluorescence [19].

Quencher induced HSA fluorescence quenching possibly classified as static/dynamic. Dynamic: Faster diffusion causes the larger collision amounts at enhanced temperatures thereby increased quenching constants whereas static: weaken complex stability at higher temperatures leads to reduced quenching constants.

To analyze the ETP-HSA system's fluorescence quenching, in addition to Stern-Volmer Equation (2) a modified Equation (4) was exploited and are summarized in Table 3.

$$F_0/F = 1 + k_q \tau_0 [Q] = 1 + K_{SV} [Q] \quad (2)$$

$$k_q = K_{SV}/\tau_0 \quad (3)$$

$$F_0/(F_0 - F) = (1/f_a) + (1/K_a f_a [Q]) \quad (4)$$

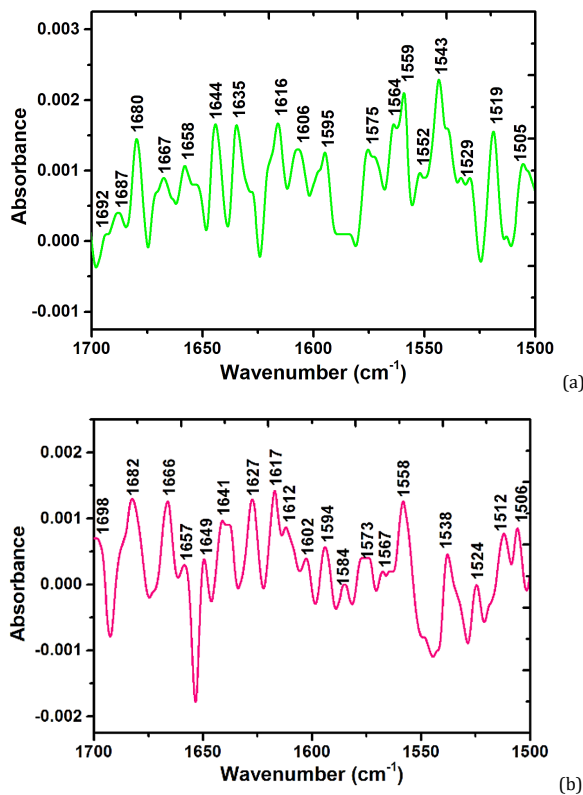


**Figure 3.** FT-IR spectra at 304 K: (a) HSA alone and (b) ETP bounded to HSA.  $c(\text{HSA}) = c(\text{ETP}) = 2.70 \times 10^{-6} \text{ mol/L}$ .

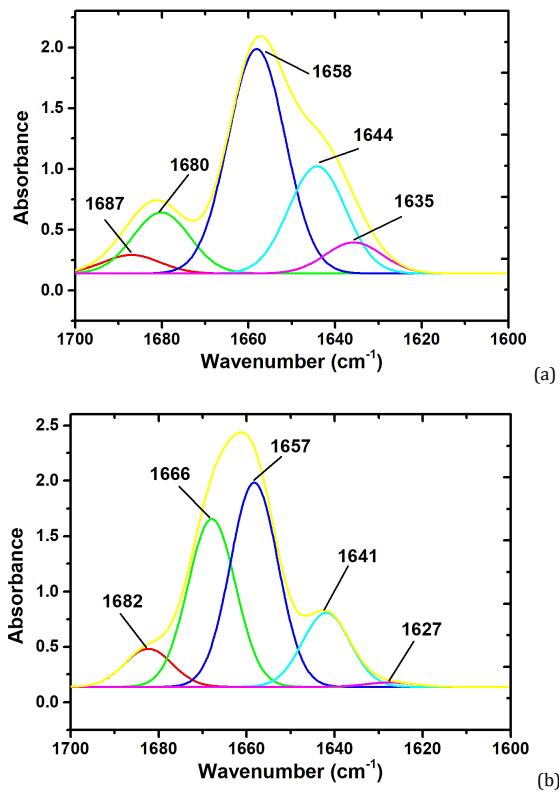


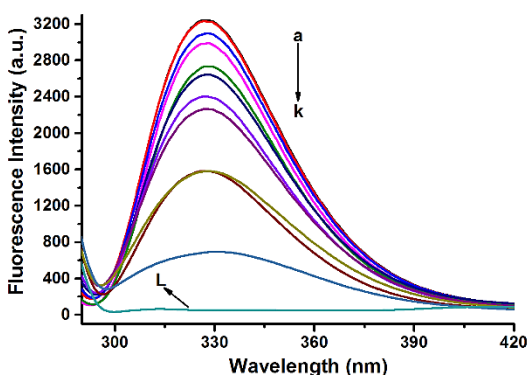
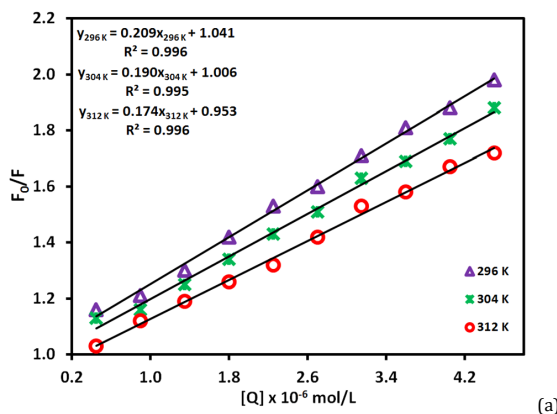
**Figure 4.** Curve fitting for (a) Free HSA and (b) ETP-HSA system at amide I band.

where,  $F_0$  is fluorescence intensity without ETP,  $F$  is fluorescence intensity with ETP,  $k_q$  is quenching rate constant,  $\tau_0$  is HSA average life time without ETP ( $\sim 2.7 \times 10^{-9} \text{ s}$ ),  $K_{SV}$  is Stern-Volmer quenching constant and  $[Q]$  is ETP concentration.

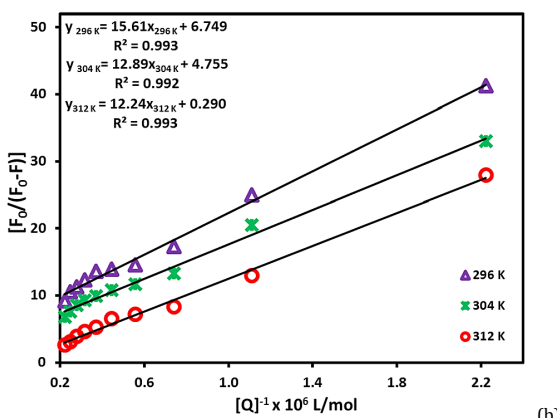
$K_a$  is effective static quenching constant and  $f_a$  is fluorophore fraction.

**Table 3.** Quenching constants to ETP-HSA system.

Temperature (K)	$K_{SV} (\text{L/mol}) \times 10^4$	$k_q (\text{L/mol.s}) \times 10^{13}$	$K_a (\text{L/mol}) \times 10^5$
296	20.9±0.05	7.74±0.03	4.32±0.10
304	19.0±0.09	7.03±0.02	3.69±0.01
312	17.4±0.04	6.44±0.02	0.24±0.08

**Figure 5.** HSA ( $2.70 \times 10^{-6}$  mol/L) fluorescence emission spectrum in distinct amounts of ETP (0 to  $4.50 \times 10^{-6}$  mol/L), curve L is ETP alone ( $2.70 \times 10^{-6}$  mol/L) at 304 K.

(a)



(b)

**Figure 6.** Plots for ETP-HSA system: (a) Stern-Volmer and (b) Modified Stern-Volmer at 296, 304 and 312 K.

$K_{SV}$  from slope of plot  $F_0/F$  versus  $[Q]$  and  $k_q$  at 296, 304 and 312 K diminished to higher temperatures (Table 3 and Figure 6a). Also,  $k_q$  values from Equation (3) are more comparable to  $2.0 \times 10^{10}$  L/mol.s (limiting diffusion rate constant) which established that static quenching (predominant ETP-HSA complex formation) [20]. This result is well supported from evaluated  $K_a$  values (lowered at raised temperatures) of modified Stern-Volmer plot (Table 3 Figure 6b) [21,22].

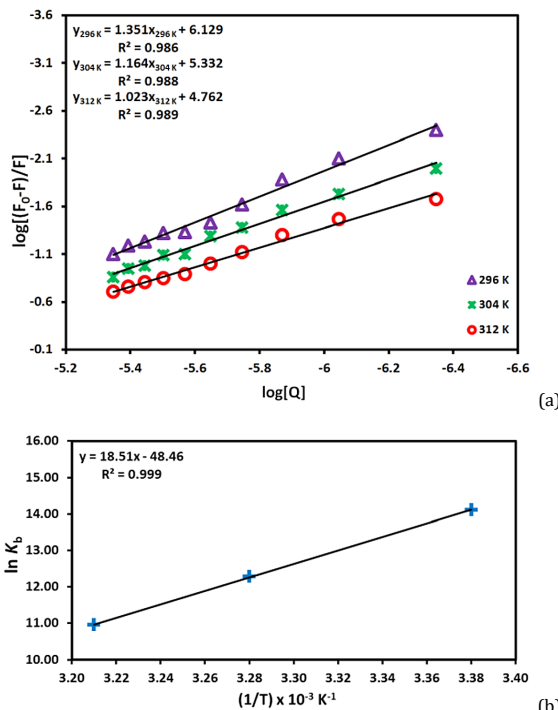
### 3.4. Binding characteristics

Drugs exist in fringe flow with protein as unbound and bound which follow the guideline of reversible equilibrium and the mass action law. Typically, for any provided drug, bound-protein and free drug always there is equilibrium. This is defined by accompanying Equation (5),

$$\log [(F_0 - F)/F] = \log K_b + n \log [Q] \quad (5)$$

**Table 4.** Binding and thermodynamic specifics for ETP-HSA interaction.

Temperature (K)	$K_b \times 10^5$ (L/mol)	n	$\Delta G$ (kJ/mol)	$\Delta H$ (kJ/mol)	$\Delta S$ (J/mol.K)
296	13.46±0.03	1.351±0.06	-34.63±0.02	-153.8±0.07	-402.9±0.08
304	2.15±0.02	1.164±0.03	-31.41±0.10		
312	0.58±0.07	1.023±0.04	-28.19±0.05		

**Figure 7.** Plots for ETP-HSA system: (a)  $\log[(F_0 - F)/F]$  versus  $\log[Q]$  and (b) van't Hoff at 296, 304 and 312 K.

The intercept gives  $K_b$  (binding constant) and slope imparts n (number of binding sites) values from the plot  $\log[(F_0 - F)/F]$  versus  $\log[Q]$  (**Table 4** and **Figure 7a**).

In plasma,  $K_b$  determines the drug's degree of circulation: Strong binding could diminish the free drug concentration, making it not accessible for the component of activity whereas weak binding prompt to poor distribution or short lifetime [23].

More affinity ETP-HSA binding ( $K_b$  of order  $10^5$ ) was reduced when decreasing in  $K_b$  was observed at raised temperatures. Assumed that this *in vitro* study is might be similar to *in vivo* study when going to perform [24,25].

Since,  $n=1.351, 1.164$  and  $1.023$  at  $296, 304$  and  $312$ , respectively, representing that the molecular population of ETP decreased in HSA binding interaction at higher temperatures. Obviously,  $n$  values were roughly 1 evincing that existence of one ETP to bind HSA.

### 3.5. Binding and thermodynamic attributes

Responsible foremost interactive forces (electrostatic, van der Waals, hydrophobic and hydrogen bonds) in ligands to proteins binding could be manifesting from thermodynamic parameters specifically changes in enthalpy ( $\Delta H$ ), free energy ( $\Delta G$ ) and entropy ( $\Delta S$ ).

Gathered binding data at 296, 304 and 312 K were utilized to explore the thermodynamic parameters from Equations (6) and (7) [26].

$$\ln K_b = (-\Delta H/RT) + (\Delta S/R) \quad (6)$$

$$\Delta G = \Delta H - T\Delta S \quad (7)$$

Linear interrelation between  $\ln K_b$  and  $1/T$  determined the values of  $\Delta S$  and  $\Delta H$  in ETP-HSA system (**Table 4** and **Figure 7b**). The evaluated values in minus  $\Delta H$ ,  $\Delta G$  and  $\Delta S$  suggested van der Waals forces with exothermic, spontaneity and hydrogen bonding, respectively, for ETP-HSA interaction. Furthermore, this ETP-HSA binding proceeded by entropy driven ( $\Delta H < \Delta S$ ).

### 3.6. Synchronous fluorescence estimations

For Tyr/Trp ( $\Delta\lambda = 15/60$  nm) synchronous fluorescence spectra in HSA when ETP varied concentration are designated in **Figure 8**. Emission maxima of Trp (**Figure 8b**) have red shift (~11 nm) which manifested that the modification in HSA conformation; increment in polarity by diminished hydrophobicity around Trp [27]. Simultaneously, Tyr emission maximum (**Figure 8a**) is reduced regularly, yet no significant wavelength change was detected. It recommends the ETP interaction with HSA doesn't influence the conformational Tyr micro-region.

### 3.7. Energy transfer assessments

Apparently, a theory named Förster's energy transfer relates energy transfer efficiency ( $E$ ) and distance ( $r$ ) between ETP and HSA is defined by Equation (8).

$$E = R_0^6 / (R_0^6 + r^6) = (F_0 - F) / F_0 \quad (8)$$

The acquired  $E$  value is 0.067. Overlapping integral ( $J$ ) for ETP and HSA is attributed as,

$$J = \{\sum [F_d(\lambda)\varepsilon_a(\lambda)\lambda^4\Delta\lambda]\} / \{\sum [F_d(\lambda)\Delta\lambda]\} \quad (9)$$

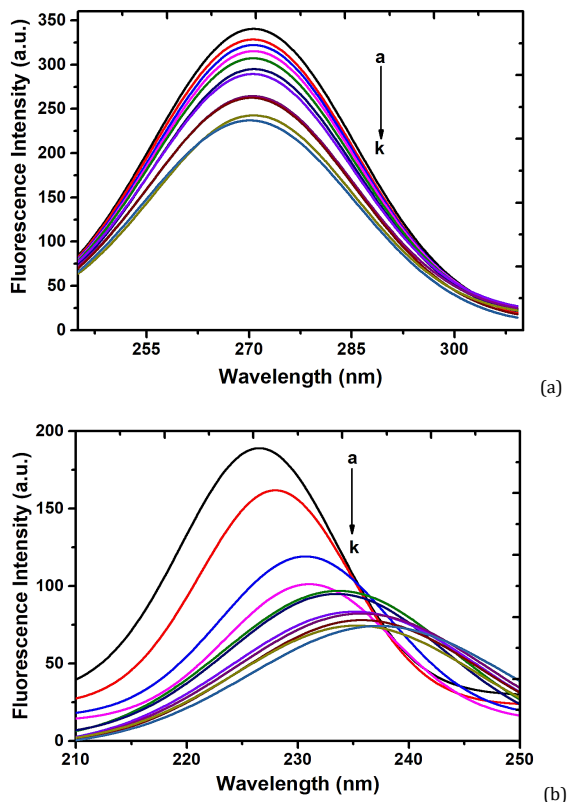


**Figure 8.** Synchronous fluorescence spectra of HSA ( $2.70 \times 10^{-6}$  mol/L) after interaction with ETP (0.0 to  $4.50 \times 10^{-6}$  mol/L): (a) Tyr and (b) Trp at 304 K.

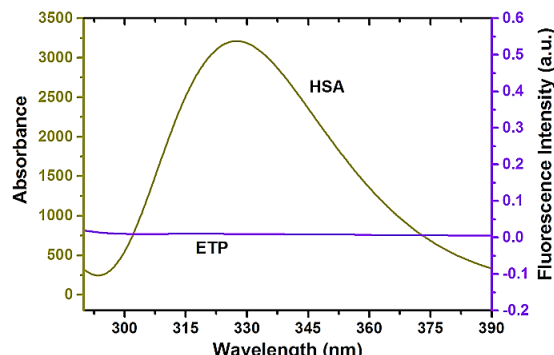


**Figure 9.** Overlapped HSA ( $2.70 \times 10^{-6}$  mol/L) fluorescence emission and ETP ( $2.70 \times 10^{-6}$  mol/L) UV-vis absorption spectrum at 304 K.

where,  $F_d(\lambda)$  and  $\varepsilon_d(\lambda)$  are fluorescence intensity of HSA and molar absorption coefficient of ETP at  $\lambda$ , respectively.  $J$  is obtained as  $1.14 \times 10^{-14}$  cm<sup>3</sup>.L/mol (from Figure 9).  $R_0$  (Critical distance) about excitation energy of 50% is transferred to ETP which is evaluated from Equation (10):

$$R_0^6 = 8.8 \times 10^{-25} K^2 N^{-4} \Phi J \quad (10)$$

In the current case,  $K^2$  (2/3),  $\Phi$  (0.15) and  $N$  (1.36) are dipole spatial orientation element, HSA fluorescence quantum yield and medium's refractive index, respectively. Found  $R_0$  is 0.26 Å. From  $E$  and  $R_0$  values, calculated  $r$  is 0.41 Å. These consequences indicate that ETP to HSA binding reaction is *via* energy transfer, which offers to static quenching ( $R_0 < r$ ) [28].

### 3.8. Metal ions on ETP binding to HSA

Abundant elements like organic, inorganic and metal ions (trace and essential) in plasmatic fluid are well predictable in

diverse biological processes. The accurate body functions are supervised by trace elements at chemical, biological and molecular forms. Several inorganic ligands and metal ions execute crucial part in medicinal diagnosis and therapy. Required  $\text{Ca}^{2+}$ ,  $\text{Co}^{2+}$ ,  $\text{Na}^+$ ,  $\text{Mg}^{2+}$  and  $\text{Fe}^{3+}$  ions portray greater affinity in relation to protein where assorted functions of metallo enzymes, organs and metabolic processes are played.  $K_b$  values of ETP-HSA system in presence of  $\text{Ca}^{2+}$ ,  $\text{Co}^{2+}$ ,  $\text{Na}^+$ ,  $\text{Mg}^{2+}$  and  $\text{Fe}^{3+}$  ions were evaluated from Equation (5) (Table 5 and Figure 10a).  $\text{Co}^{2+}$ ,  $\text{Mg}^{2+}$  and  $\text{Fe}^{3+}$  ions diminished  $K_b$  values of ETP-HSA system where these ions decrease the ETP binding with HSA and lower the ETP accumulation in blood for long period.

Increased  $K_b$  values implied the formation of ETP-metal ion-HSA stable complexes across metal ion bridge for  $\text{Ca}^{2+}$  and  $\text{Na}^+$  ions. Hence, presence of  $\text{Ca}^{2+}$  and  $\text{Na}^+$  ions might boost the delivery exploit of ETP to the target spot by prolonging its storage time.

**Table 5.** Binding constants to ETP-HSA system with metal ions and site probes at 304 K.

System	$K_b$ (L/mol) *
HSA-ETP	$2.15 \pm 0.06 \times 10^5$
HAS-ETP-Ca <sup>2+</sup>	$3.56 \pm 0.07 \times 10^5$
HSA-ETP-Co <sup>2+</sup>	$1.02 \pm 0.01 \times 10^4$
HSA-ETP-Na <sup>+</sup>	$1.71 \pm 0.04 \times 10^6$
HSA-ETP-Mg <sup>2+</sup>	$2.44 \pm 0.06 \times 10^3$
HSA-ETP-Fe <sup>3+</sup>	$1.84 \pm 0.10 \times 10^2$
HAS-ETP-Warfarin	$1.82 \pm 0.09 \times 10^5$
HAS-ETP-Ibuprofen	$1.88 \pm 0.01 \times 10^4$
HAS-ETP-Digitoxin	$1.46 \pm 0.03 \times 10^5$

\*  $K_b$  is binding constant.

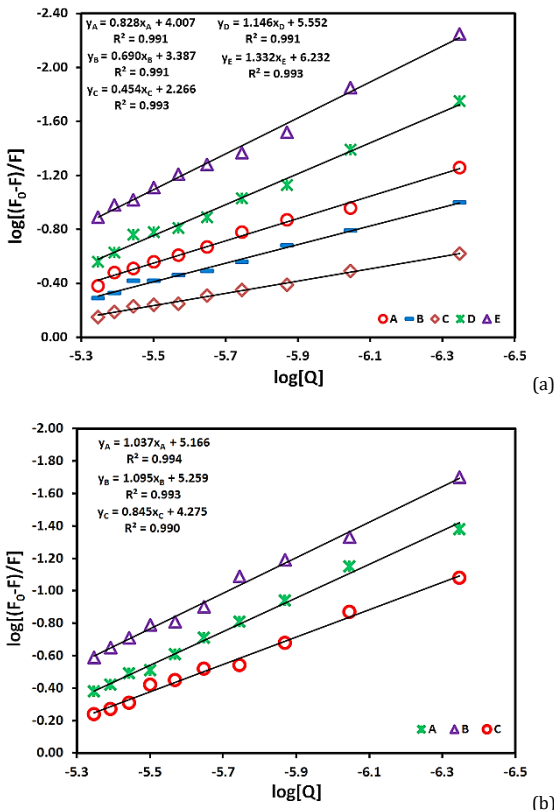


**Figure 10.** Binding constants to ETP-HSA system (a) with (A-Co<sup>2+</sup>, B-Mg<sup>2+</sup>, C-Fe<sup>3+</sup>, D-Ca<sup>2+</sup> and E-Na<sup>+</sup>) and (b) with (A-Ibuprofen, B-Warfarin and C-Digitoxin) at 304 K.

Subsequently these aspects assist in regulating the ETP dose limits for successful treatment and in accomplishing the ideal therapeutic outcomes [29].

### 3.9. ETP selective site binding

Drug competitive nature affects the bound and unbound drug concentration in HSA to bind compatible site [30]. The estimated  $K_b$  values from Equation (5) for each site markers on ETP-HSA system's binding affinity is supplied in Table 5 and Figure 10b. The subsequent altered  $K_b$  value for ibuprofen in contrast to other two from Table 5 intimates that ETP effectively competed with ibuprofen for site II (IIIA) by relocating ibuprofen from its posture.

### 3.10. Molecular docking examinations

Docking speculates the best fit inclination of ETP where it goes and proceeds to bind HSA to frame stable complex. Cluster analysis for individual binding sites were done using 2.0 Å RMSD tolerance to 80 docking runs (Figure 11 and Table 6) with lowest average binding energy received to site II [31]. This is energetically finest favorable ETP conformation immediately bound to HSA. Less  $E_{vdw+HB+deso}$  value contrasted with  $E_{Elec}$  (Table

7) associated to hydrogen bonds bearing van der Waals comprised for HSA and ETP binding at site II (IIIA).

### 3.11. Three-dimensional fluorescence

HSA conformational modulations upon ETP binding is thoroughly investigated from 3D fluorescence. Figure 12 depicts the 3D fluorescence spectra of bound ETP and free HSA which demonstrating 4 peaks namely 'a' portraying first-order ( $\lambda_{em} = \lambda_{ex}$ ), 'b' illustrating second-order ( $\lambda_{em} = 2\lambda_{ex}$ ) Rayleigh scattering, '1' designating aromatic amino acids (Tyr/Trp:  $n \rightarrow \pi^*$  transition) and '2' denoting polypeptide sequence ( $\pi \rightarrow \pi^*$  transition) [32]. On binding with ETP, substantial reduction in peak intensities was noticed for HSA (Table 8) signifying the alterations in polypeptide framework and Trp/Tyr micro-environment.

## 4. Conclusions

ETP binding characteristics with HSA was schematically investigated from spectroscopic tools. ETP subsequently quenched the HSA across static with ETP-HSA complex formation.

**Table 6.** Docking results to ETP-HSA system at distinct sites

Binding site	Interactions		Distance (Å)	Amino acid-ETP atom
	Type			
Site I (IIA)	van der Waals	-	SER287	
		-	VAL241	
		-	ILE264	
		-	HIS247	
		-	GLN196	
		-	TRP214	
		-	LEU219	
		-	LEU238	
	Conventional Hydrogen Bond	2.19	ARG257:HE-01	
		1.96	ARG257:HH22-O2	
		3.59	GLU292:OE1-C7	
		3.72	ARG222:NH2-aromatic ring 3	
		3.38	ARG222:NH1-aromatic ring 2	
		4.06	LYS199: NZ-aromatic ring 2	
		2.71	LYS199: NZ-aromatic ring 3	
		3.80	ILE290:CG2-aromatic ring 1	
	Pi-Cation	5.50	LYS199:(CB-CG-CD)-ring	
		5.04	ALA291:CB-aromatic ring 2	
		5.23	ALA291:CB-aromatic ring 1	
		5.07	ARG257:(CB-CG)-aromatic ring 1	
		4.27	ALA261:(CB)-aromatic ring 1	
		4.78	LEU260:(CB-CG-CD2)-aromatic ring 1	
		5.25	ARG218:(CB-CG)-aromatic ring 1	
		5.47	ARG218:(CB-CG)-aromatic ring 2	
Site II (IIIA)	van der Waals	-	GLU492	
		-	SER489	
		-	LEU387	
		-	ASN391	
		-	GLN390	
		-	PHE403	
		-	LEU407	
		-	LYS413	
	Conventional Hydrogen Bond	1.89	LYS414:HZ2-O1	
		1.69	LYS414:HZ1-O2	
		1.64	ARG410:HE-02	
		2.69	ARG410:HH21-O2	
		2.90	LEU491:O-01	
		4.83	ARG410:aromatic ring 2-(CG-CB)	
		4.49	ARG410:aromatic ring 3-(CG-CB)	
		5.11	ALA406:CB - aromatic ring 3	
	Unfavorable Acceptor-Acceptor	5.32	LEU394:(CD1-CG-CD2)-aromatic ring 3	
		5.43	VAL409:(CG2-CB-CG1)-ring	
		3.30	ARG410:NH1-aromatic ring 3	
		3.38	ARG410:NH1-aromatic ring 1	
Site III (IB)	van der Waals	-	LYS137	
		-	GLU141	
		-	ARG117	
		-	PRO118	
		-	MET123	
		-	TYR161	
		-	VAL116	
		-	HIS146	
		-	LYS190	
	Conventional Hydrogen Bond	2.26	TYR138: OH-H15	
		3.55	LEU115:CD2-aromatic ring 1	
		3.55	ILE142:CD1-aromatic ring 3	
		5.13	TYR138:aromatic ring-aromatic ring 1	
		4.14	LEU185:C-aromatic ring 3	
		5.33	LEU182:(CD1-CG-CD2)-aromatic ring 2	
		5.44	LEU115:(CD1-CB-CG)-ring	
		4.88	ARG145:(CG-CB)-ring	
		4.74	ILE142:(CG1-CB-CG2)-ring	
Pi-Alkyl	Pi-Alkyl	4.06	ARG186:(CG-CG)-aromatic ring 3	
		3.72	ARG186: (CB-CG)-aromatic ring 2	

**Table 7.** Diverse energies to ETP-HSA system from Lamarckian Genetic Algorithm.\*

Rank	Run	$\Delta G$ (kJ/mol)	$E_{inter-mol}$ (kJ/mol)	$E_{vdw+HB+desol}$ (kJ/mol)	$E_{elec}$ (kJ/mol)
1	8	-37.95	-45.44	-43.81	-1.67
2	78	-36.44	-43.92	-43.30	-0.67
3	16	-36.19	-43.68	-42.68	-1.00
4	69	-35.77	-43.26	-42.59	-0.67
5	41	-32.30	-39.79	-38.70	-1.09

\*  $\Delta G$  is the binding free energy,  $E_{inter-mol}$  is the intermolecular interaction energy; sum of Vander Waals energy, hydrogen bonding energy, desolvation free energy and electrostatic energy,  $E_{vdw+HB+desol}$  is the sum of Vander Waals energy, hydrogen bonding energy and desolvation free energy,  $E_{elec}$  is the electrostatic energy.

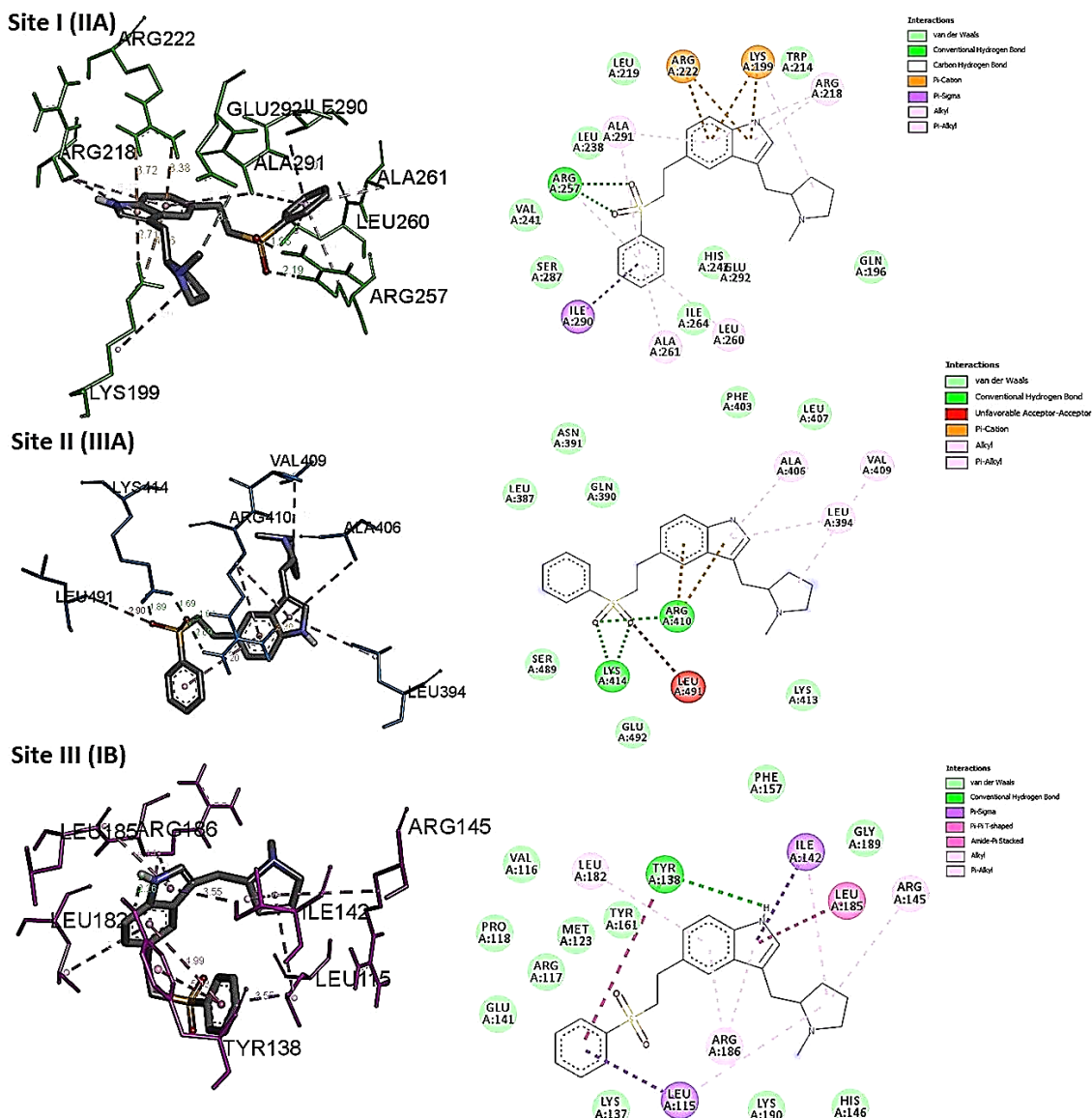


Figure 11. Numerous binding sites depicted to ETP docked with HSA.

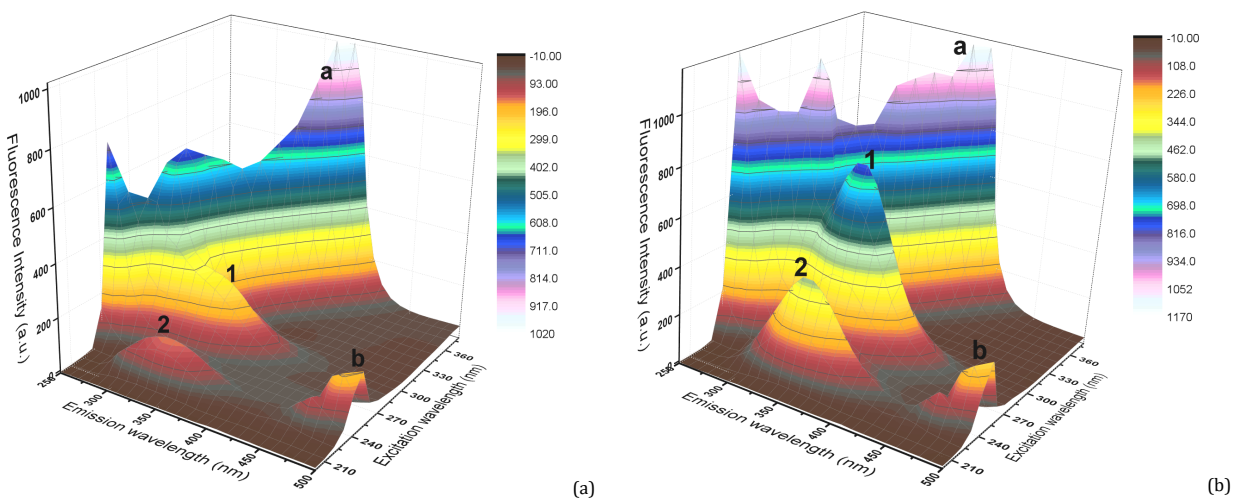


Figure 12. 3D fluorescence spectra: (a) HSA only and (b) ETP-HSA system.

**Table 8.** At 304 K, 3D fluorescence aspects: free HSA and ETP-HSA system.

Peak position (λ <sub>ex</sub> /λ <sub>em</sub> , nm/nm)	Peak	Intensity Free HSA	HSA-ETP
270/270 → 370/370	a	683.4 → 1141	741.7 → 1006
250/500	b	269	199.6
280/340	1	779.3	278.2
230/340	2	417.3	154.2

The achieved results supported the Trp micro-environment alterations and HSA secondary structure modifications. Hydrogen bonds grouping with van der Waals are validated from thermodynamic constituents to stabilize ETP-HSA system through spontaneously. Best configuration of HSA showed site II for ETP binding. The gained data from present examination can aid in exploring the pharmacodynamics and pharmacokinetics specificities of those significant serotonin agonist drugs.

### Acknowledgements

Manjushree Makegowda thanks to University Grants Commission of Basic Scientific Research (UGC-BSR) for awarding the Senior Research Fellowship (SRF) under meritorious students and Institute of Excellence (IOE), Vijnana Bhavan, Mysuru for instrumental assistances.

### Disclosure statement

Conflict of interests: The authors declare that they have no conflict of interest.

Author contributions: All authors contributed equally to this work.

Ethical approval: All ethical guidelines have been adhered.

Sample availability: Samples of the compounds are available from the author.

### ORCID

Manjushree Makegowda

 <http://orcid.org/0000-0003-0298-4333>

Revanasiddappa Hosakere Doddarevanna

 <http://orcid.org/0000-0003-0127-3599>

### References

- [1]. Migraine, Wikipedia, <https://en.wikipedia.org/wiki/Migraine>, 2020 (Accessed 11 February 2020).
- [2]. Eletriptan-hydrochloride, NPS Medicinewise, <https://www.nps.org.au/australian-prescriber/articles/eletriptan-hydrochloride>, 2020 (Accessed 11 February 2020).
- [3]. Eletriptan, Wikipedia, <https://en.wikipedia.org/wiki/Eletriptan>, 2020 (Accessed 11 February 2020).
- [4]. Kremer, J. M.; Wilting, J.; Janssen, L. H. *Pharmacol. Rev.* **1988**, *40*, 1-47.
- [5]. Ghuman, J.; Zunszain, P. A.; Petitpas, I.; Bhattacharya, A. A.; Otagiri, M.; Curry, S. *J. Mol. Biol.* **2005**, *353*, 38-52.
- [6]. Fasano, M.; Curry, S.; Terreno, E.; Galliano, M.; Fanali, G.; Narciso, P.; Notari, S.; Ascenzi, P. *IUBMB Life* **2005**, *57*, 787-796.
- [7]. Zolfaghzaradeh, M.; Pirouzi, M.; Asoodeh, A.; Saberi, M. R.; Chamani, J. *J. Biomol. Struct. Dyn.* **2013**, *32*, 1936-1952.
- [8]. Kamshad, M.; Shah Talab, M.; Beigoli, S.; Sharifi, R. A.; Chamani, J. *J. Biomol. Struct. Dyn.* **2018**, *37*, 2030-2040.
- [9]. Manjushree, M.; Revanasiddappa, H. D. *Spectrochim. Acta A* **2019**, *209*, 264-273.
- [10]. Sanei, H.; Asoodeh, A.; Hamedakbari-Tusi, S.; Chamani, J. *J. Solution Chem.* **2011**, *40*, 1905-1931.
- [11]. Ariga, G. G.; Naik, P. N.; Nandibewoor, S. T.; Chimataradar, S. A. *J. Biomol. Struct. Dyn.* **2016**, *35*, 3161-3175.
- [12]. Manjushree, M.; Revanasiddappa, H. D. *Bioinorg. Chem. Appl.* **2018**, *6954951*, 1-13.
- [13]. Mokaberi, P.; Reyhani, V.; Amiri-Tehranizadeh, Z.; Saberi, M. R.; Beigoli, S.; Samandar, F.; Chamani, J. *New J. Chem.* **2019**, *43*, 8132-8145.
- [14]. Sharif-Barfeh, Z.; Beigoli, S.; Marouzi, S.; Rad, A. S.; Asoodeh, A.; Chamani, J. *J. Solution Chem.* **2017**, *46*, 488-504.
- [15]. Manjushree, M.; Revanasiddappa, H. D. *Chem. Phys.* **2020**, *530*, 110593.
- [16]. Shakibapour, N.; Dehghani Sani, F.; Beigoli, S.; Sadeghian, H.; Chamani, J. *J. Biomol. Struct. Dyn.* **2018**, *37*, 359-371.
- [17]. Yue, Y.; Sun, Y.; Dong, Q.; Liu, R.; Yan, X.; Zhang, Y.; Liu, J. *Luminescence* **2016**, *31*, 671-681.
- [18]. Yue, Y.; Liu, J.; Liu, R.; Sun, Y.; Li, X.; Fan, J. *Food Chem. Toxicol.* **2014**, *71*, 244-253.
- [19]. Bourassa, P.; Dubeau, S.; Maharvi, G. M.; Fauq, A. H.; Thomas, T. J.; Tajmir-Riahi, H. A. *Biochimie* **2011**, *93*, 1089-1101.
- [20]. Abdelhameed, A. S.; Alam, P.; Khan, R. H. *J. Biomol. Struct. Dyn.* **2016**, *159*, 199-208.
- [21]. Sohrabi, T.; Hosseinzadeh, M.; Beigoli, S.; Saberi, M. R.; Chamani, J. *J. Mol. Liq.* **2018**, *256*, 127-138.
- [22]. Chamani, J.; Vahedian-Movahed, H.; Saberi, M. R. *J. Pharmaceut. Biomed.* **2011**, *55*, 114-124.
- [23]. Feroz, S. R.; Mohamad, S. B.; Bujang, N.; Malek, S. N.; Tayyab, S. *J. Agric. Food Chem.* **2012**, *60*, 5899-5908.
- [24]. Dehghani Sani, F.; Shakibapour, N.; Beigoli, S.; Sadeghian, H.; Hosainzadeh, M.; Chamani, J. *J. Lumin.* **2018**, *203*, 599-608.
- [25]. Moosavi-Movahedi, A.; Chamani, J.; Gharanfoli, M.; Hakimelahi, G. *Thermochim. Acta* **2004**, *409*, 137-144.
- [26]. Abdelhameed, A. S.; Alanazi, A. M.; Bakheit, A. H.; Darwish, H. W.; Ghabbour, H. A.; Darwish, I. A. *Spectrochim. Acta A* **2017**, *171*, 174-182.
- [27]. Jirgensons, B. *J. Biol. Chem.* **1965**, *240*, 1064-1071.
- [28]. Weiss, S. *Science* **1999**, *283*(5408), 1676-1683.
- [29]. Roy, A. S.; Tripathy, D. R.; Chatterjee, A.; Dasgupta, S. *Spectrochim. Acta A* **2013**, *102*, 393-402.
- [30]. Jacobsen, J.; Brodersen, R. *J. Biol. Chem.* **1983**, *258*, 6319-6326.
- [31]. Sharifi-Rad, A.; Mehrzad, J.; Darroudi, M.; Saberi, M. R.; Chamani, J. *J. Biomol. Struct. Dyn.* **2020**, 1-27.
- [32]. Guo, X. J.; Sun, X. D.; Xu, S. K. *J. Mol. Struct.* **2009**, *931*, 55-59.



Copyright © 2020 by Authors. This work is published and licensed by Atlanta Publishing House LLC, Atlanta, GA, USA. The full terms of this license are available at <http://www.eurjchem.com/index.php/eurjchem/pages/view/terms> and incorporate the Creative Commons Attribution-Non Commercial (CC BY NC) (International, v4.0) License (<http://creativecommons.org/licenses/by-nc/4.0/>). By accessing the work, you hereby accept the Terms. This is an open access article distributed under the terms and conditions of the CC BY NC License, which permits unrestricted non-commercial use, distribution, and reproduction in any medium, provided the original work is properly cited without any further permission from Atlanta Publishing House LLC (European Journal of Chemistry). No use, distribution or reproduction is permitted which does not comply with these terms. Permissions for commercial use of this work beyond the scope of the License (<http://www.eurjchem.com/index.php/eurjchem/pages/view/terms>) are administered by Atlanta Publishing House LLC (European Journal of Chemistry).